AD NUMBER
AD914575
LIMITATION CHANGES
TO: **Approved for public release; distribution is unlimited.**
FROM: **Distribution authorized to U.S. Gov't. agencies only; Test and Evaluation; NOV 1973. Other requests shall be referred to Office of Naval Research, Attn: 421, Arlington, VA 22217.**
AUTHORITY
ONR ltr, 8 Oct 1975

CW PIN DISCHARGE LASER

Final Technical Report
November 14, 1973

Sponsored by
Advanced Research Projects Agency
ARPA Order No. 1806

under

Contract No. N00014-73-C-0318

Scientific Officer: Director, Physics Program
Physical Sciencies Division
Office of Naval Research
Department of Navy
800 North Quincy Street
Arlington, Virginia 22217

Program Code No. 3E90
Amount of Contract: $99,980
Effective Date of Contract: March 15, 1973
Contract Expiration Date: September 14, 1973
Principal Investigator: S. A. Wutzke
Phone No. (412) 256-3252
Authors: S. A. Wutzke, J. L. Pack, G. L. Rogoff,
J. J. Lowke

Westinghouse Research Laboratories
PITTSBURGH, PENNSYLVANIA 15235

CW PIN DISCHARGE LASER

Final Technical Report
November 14, 1973

Sponsored by
Advanced Research Projects Agency
ARPA Order No. 1806

under

Contract No. N00014-73-C-0318

Scientific Officer: Director, Physics Program
Physical Sciencies Division
Office of Naval Research
Department of Navy
800 North Quincy Street
Arlington, Virginia 22217

Program Code No. 3E90
Amount of Contract: $99,980
Effective Date of Contract: March 15, 1973
Contract Expiration Date: September 14, 1973
Principal Investigator: S. A. Wutzke
Phone No. (412) 256-3252
Authors: S. A. Wutzke, J. L. Pack, G. L. Rogoff,
J. J. Lowke

TABLE OF CONTENTS

CW PIN DISCHARGE LASER

S. A. Wutzke, J. L. Pack, G. L. Rogoff and J. J. Lowke
Westinghouse Research Laboratories
Pittsburgh, Pennsylvania 15235

ABSTRACT

The results of a study program on a Continuously Operating Fast Flow Electrically Excited (COFFEE) laser excitation concept are reported. The concept uses a multipin-to-plane electrode configuration with transverse gas flow to produce a high-pressure, self-sustained glow discharge. Emphasis is placed on developing the glow discharge scaling criteria. Both theoretical and experimental studies of the glow discharge characteristics, input power distribution, and glow-to-arc transition phenomena are described. The high-pressure continuous glow was successfully scaled experimentally to a 10 cm square aperture. The excitation concept looks attractive for high-power laser devices.

SUMMARY

This is the final technical report for Phase I of a research program supported by The Advanced Research Projects Agency of the Department of Defense and monitored by ONR under contract N00014-C-73-0318 for the period 15 March 1973 to 14 September 1973. This is the first part of a two-phase program with the objective of determining the discharge scaling criteria for the COFFEE laser excitation technique. This technique utilizes a high-pressure self-sustained glow discharge. A multipin-to-plane electrode system is used with transverse gas flow. The objectives of Phase I were met. The high-pressure continuous glow was successfully scaled to a 10 cm square aperture using a 10 x 10 x 10 cm electrode module.

The V-I characteristics were determined for a self-sustained continuous glow discharge by calculating the steady state balance between electron generation and loss mechanisms. The operating E/N was determined as a function of j/N for both the attachment and recombination dominated limits. Experimental evidence indicates that the glow is attachment controlled in the current density range of interest for the gas mixtures considered. An E/N of 2.6×10^{-16} V-cm^2 was obtained for a $1CO_2:7N_2:30He$ gas mixture which is only slightly above the optimum E/N for maximum excitation efficiency.

As the laser gas passes transversely through the glow discharge, the gas temperature rises almost linearly along the flow direction if one keeps the input power per unit volume constant. Similarly, the gas density decreases non-linearly along the flow direction which is transverse to the optical axis. The variation in gas density requires that the current density increase linearly along the flow direction in order to maintain a constant input power density. This is easily accomplished in the COFFEE laser by suitably adjusting the cathode row currents.

Specific input energies up to 115 J/ℓ-atm (110 kJ/lb) were obtained with input power densities up to 50 W/cm^3 of discharge volume using a new discharge module. Parametric optimization and the elimination of anode edge effects are expected to raise the specific input to over 200 J/ℓ-atm. No fundamental scaling limit has been encountered for electrode spacings up to 10 cm.

Glow-to-arc transitions appear to be due to local thermal instabilities. A simplified computer code was developed which follows the spatial and temporal change in electrical conductivity when a small perturbation is imposed on an initially uniform glow. These perturbations may be caused by local hot spots in the gas temperature field, for example, near the electrodes. Gas flow is an important stabilizing agent.

Additional scaling studies are recommended to provide a more definitive evaluation of the COFFEE laser scalability. Discharge parameterization experiments should be extended over broader ranges of the primary variables. Glow-to-arc transitions are a limiting factor, yet are poorly understood. Small-signal gain measurements would determine excitation efficiency and verify excitation uniformity. The recommended studies would lead to a more comprehensive laser discharge scaling criteria from which multikilowatt CO_2 lasers could easily be designed.

1. INTRODUCTION

The approach in this study program is based on the use of a Continuously Operating Fast Flow Electrically Excited (COFFEE) laser concept. The COFFEE laser uses a new high-pressure (0.1 to 1 atm) direct current self-sustained glow discharge excitation scheme which is well suited for a continuous wave CO_2 laser. The continuous glow is produced with a multipin-to-plane electrode geometry and is stabilized by a gas flow transverse to the discharge and by a ballast resistor in series with each cathode pin. A high-power CO_2 laser system using this excitation scheme would be relatively simple, rugged, compact, and inexpensive.

The objective of the program described herein has been the development of the high-pressure glow discharge scaling criteria for the multipin-to-plane electrode system. Particular emphasis has been placed on understanding the physics of the discharge as they relate to discharge scalability and laser excitation efficiency. Parallel, complementary approaches involving both theoretical modeling and experimental studies have been pursued. Specific tasks have included theoretical analysis to develop models of the discharge characteristics, input energy distribution, and discharge stability as described in Section 2. The experimental tasks have included the construction and testing of an electrode module (10 x 10 x 10 cm) to measure the important glow discharge parameters as described in Section 3. The study program is a two-phase program, and the results being reported summarize the status of the the program at the end of Phase I.

2. THEORETICAL MODELING

2.1 V-I Characteristics

The COFFEE laser excitation scheme uses a continuous self-sustained glow discharge in high-pressure CO_2 laser gas mixtures. The power into the discharge is governed by the voltage-current characteristics of the glow while the operating E/N, ratio of electric field to neutral gas density, controls the laser excitation efficiency.[1] It is important, therefore, to determine what factors govern these parameters.

The operating E/N of a glow discharge is that value which leads to a steady state balance between the rates of all the electron generation and loss mechanisms. The analysis of Lowke, Phelps, and Irwin[2] shows that for a volume controlled discharge

$$j/N = (eW^2/\gamma)(\alpha-a)/N \qquad (2\text{-}1)$$

where j is the current density, N is the neutral gas density, e is the electron charge, W is the electron drift velocity, γ is the recombination loss rate, α is the ionization coefficient, and a is the attachment coefficient. Equation (2-1) expresses j/N as a function of E/N through the dependences calculated by Lowke et al. of W, α/N, and a/N on E/N. The curves in Fig. 1 were drawn for Eq. (2-1) using three representative gas mixtures. For low values of j/N two limits are shown. The broken curves correspond to the case of an attachment dominated glow while the solid curves correspond to a recombination controlled glow. Gases such as CO_2, H_2O, and O_2 are known to produce electron loss by attachment.[3] For example, dissociative attachment by CO_2 to form CO and O^- leads to electron loss. The addition of 1% water vapor to the laser gas[4] has produced a definite increase in operating E/N. Certain gas additives[4-6] may act to suppress attachment and lower the operating E/N at a

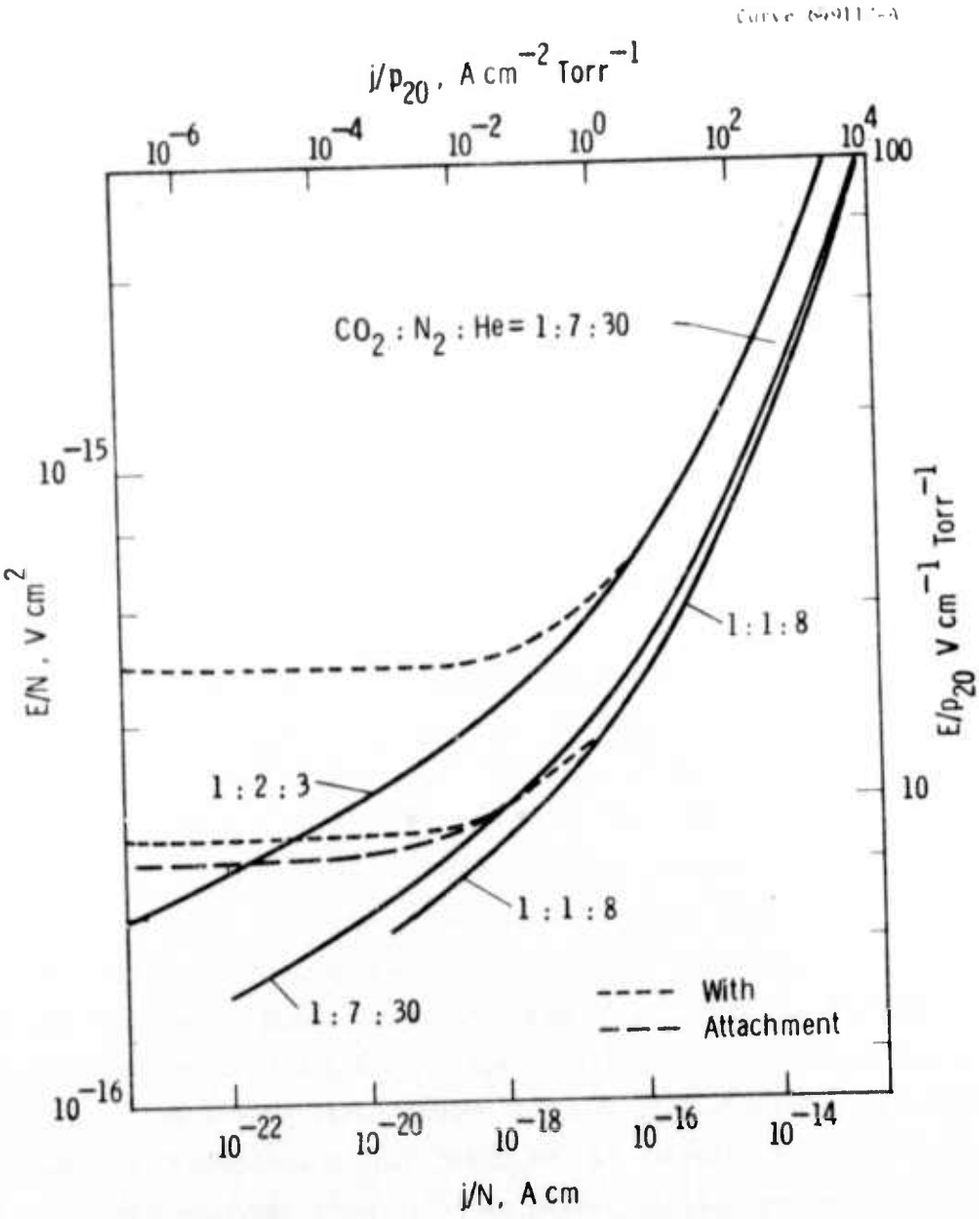

Fig. 1. Predicted E/N-j/N characteristics assuming there is a volume controlled glow with $\gamma = 10^{-7}$ cm^3 sec^{-1}.

given j/N. This would result in a slightly higher laser excitation efficiency (see Fig. 2). The operating value of E/N will become recombination-controlled at high current densities since recombination losses increase as the square of current.

The COFFEE laser operates in the current regime ($j/N < 10^{-19}$ A-cm) where attachment appears to dominate the discharge. Figure 3 shows calculated values of α/N and a/N as a function of E/N for three gas mixtures.[4] For a 1:7:30 mixture of CO_2:N_2:He the predicted operating value of E/N is 2.6×10^{-16} V-cm^2. This agrees with the results of the experiments described in Section 3. Similar data has also been obtained in the quasi-steady-state regime over a wider current range ($10^{-21} < j/N < 10^{-17}$ A-cm) using a pulsed, self-sustained discharge.[4]

The effect of varying the helium content in the laser mixture is also indicated in Fig. 2. For a given E/N, if the proportion of helium is increased, the average electron energy is also increased because helium has none of the inelastic vibrational losses that are present in N_2 and CO_2. Thus, electron energies sufficient to excite the upper laser level occur at a lower E/N for the 1:7:30 mixture than for the 1:7:0 mixture where helium is absent. The solid line in Fig. 2 shows the percentage of total power delivered to the upper laser levels. The maximum efficiency for the 1:7:30 mixture occurs at $E/N = 1.2 \times 10^{-16}$ V-cm^2 and at 4×10^{-16} V-cm^2 for the 1:7:0 mixture.

One might try to optimize, if possible, the operating E/N to obtain maximum efficiency by varying the proportion of helium. However, it is seen from Fig. 2 that the change in E/N for maximum efficiency and the change in operating E/N are approximately the same. The change will also be about the same if the discharge is recombination rather than attachment controlled. Although no account has been taken of the effect of helium in depopulating the lower laser levels, these calculations appear to demonstrate that the addition of helium has no significant influence on the effective laser excitation efficiency for a self-sustained glow discharge at a given current density. Note, however, that the excitation efficiency has a broad maxima, and self-sustained discharges operate at an E/N differing only slightly from the predicted E/N for maximum efficiency.

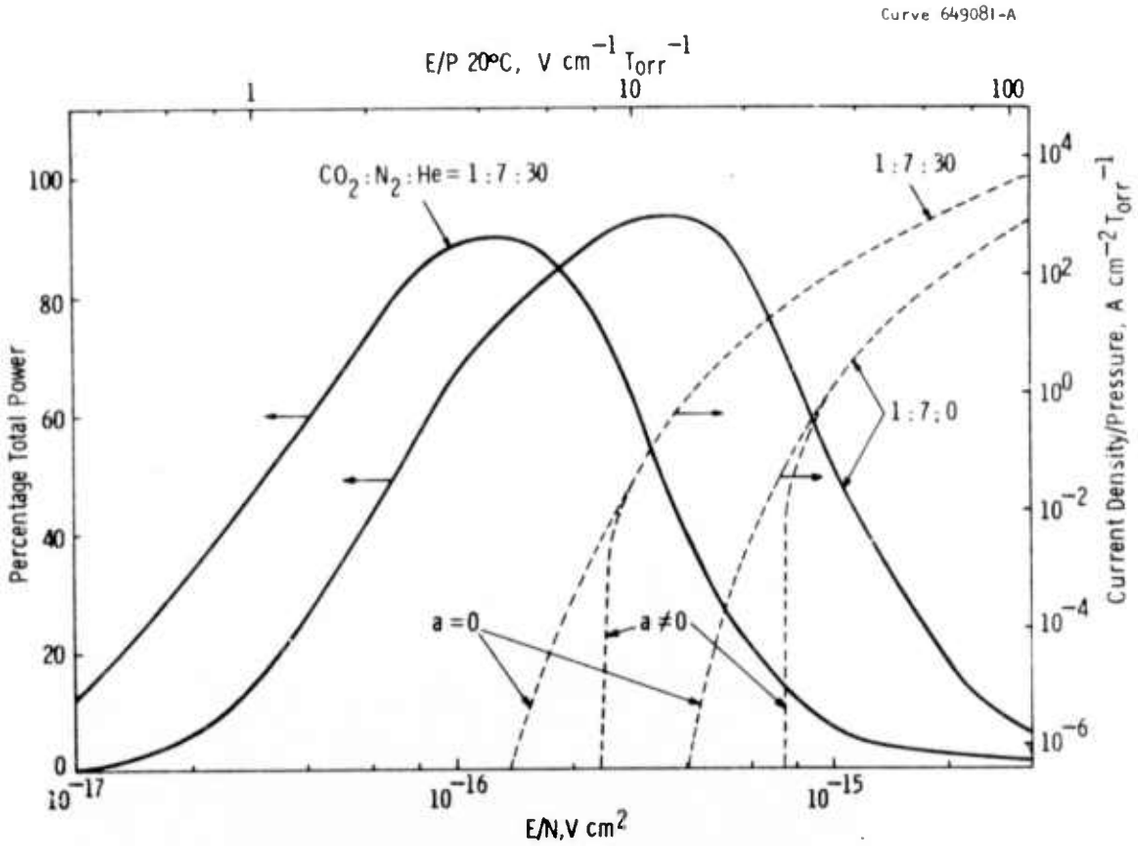

Fig. 2. Solid curves show calculated excitation efficiency based on excitation levels coupled to the upper laser level. Broken curves show calculated V-I characteristics for two laser mixtures.

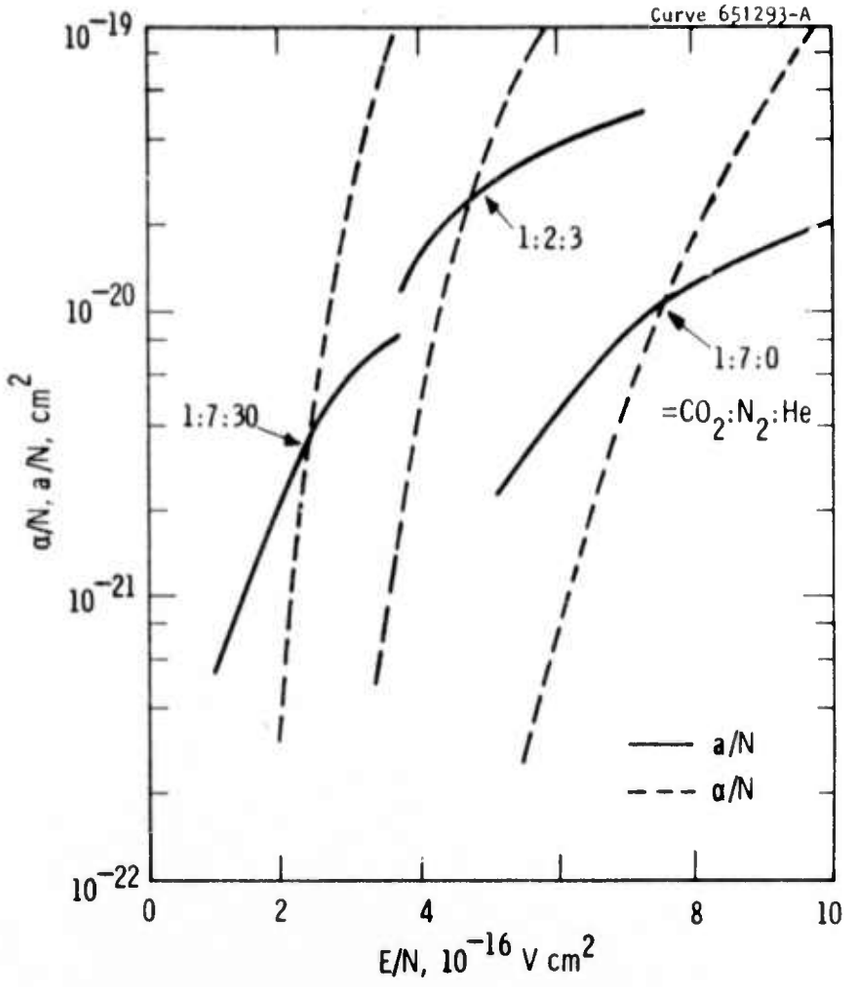

Fig. 3. Calculated values of α/N and a/N as a function of E/N for the mixtures indicated.

2.2 Input Energy Considerations

In the COFFEE laser excitation scheme the laser gas passes transversely through a self-sustained glow discharge during excitation. Some of the electrical energy put into the discharge is extracted as useful optical energy while the rest is dissipated as waste heat and increases the gas temperature. Under typical operating conditions the gas temperature rises almost linearly with displacement along the flow direction while passing through the discharge. Since changes in gas temperature directly affect many important laser parameters, such as gas density, electrical field strength, gain, and input power, it is important to understand how these quantities are related to the operating parameters of the laser.

The gas temperature rise along an incremental displacement (dx) in the flow direction is readily obtained by performing an energy balance on a small volume element. Assuming steady state and a constant cross sectional area for the flow, one obtains:

$$c_p \frac{dT_o}{dx} = (1-\eta) \frac{jE}{\rho v} \qquad (2\text{-}2)$$

where T_o is the local stagnation temperature, c_p the specific heat capacity, η the electrical-to-optical laser conversion efficiency, j the current density, E the electric field, ρ the gas density, and v the gas velocity. From mass conservation for a constant area duct

$$\rho v = \dot{m}/A = \text{const.} \qquad (2\text{-}3)$$

The product jE is the electrical power per unit volume which might have any arbitrary x dependence. However, the condition jE = const. is of special interest because this gives, assuming constant η, the desired uniform laser output condition. Upon integration of Eq. (2-2) one obtains:

$$\frac{T_o(x)}{T_o(0)} - 1 = \frac{(1-\eta)jEw}{\rho v c_p T_o(0)} \left[\frac{x}{w}\right] \qquad (2\text{-}4)$$

which can be rewritten

$$\frac{T_o(\zeta)}{T_o(0)} = 1 + \varepsilon\zeta \qquad (2\text{-}5)$$

where $\varepsilon = (1-\eta)jEw/\rho v c_p T_o(0)$ = ratio of net energy added to initial energy content of gas.

$\zeta = x/w$ = normalized distance in flow direction.

w = width of discharge channel in flow direction.

Since ε is constant, we see that the stagnation temperature increases linearly with ζ.

To determine how the other parameters, such as pressure, density, and velocity, vary with ζ, one must satisfy the remaining conservation equations. The solution to all these conditions is the well-known Rayleigh Line criteria[7] for flow in a frictionless, constant-area duct with heat addition. The initial gas velocity and rate of heat addition to the gas can be expressed in terms of the local Mach number (M) for the gas. All the other variables are then expressed in terms of M. These functions are usually tabulated or plotted against M for various values of the gas constants.

In order to visualize more easily the changes which are taking place when the laser gas is heated, it is possible to make a few simplifying assumptions which only introduce a small error into the results. First, for $M < 0.5$ the local static temperature differs from the local stagnation temperature by less than 5%. This means that the gas kinetic energy is relatively low for small M. Thus, according to Eq. (2-5), the static temperature distribution is approximated by:

$$\frac{T(\zeta)}{T_i} \simeq 1 + \varepsilon\zeta \qquad (2\text{-}6)$$

where T_i = initial gas temperature at the upstream edge of the discharge. We see that T increases linearly with ζ for the condition of constant jE.

Gas heating always reduces the gas stagnation pressure. However, for M < 0.5 at $\zeta = 1$ the total change in stagnation pressure will typically be less than 10%. Also the change in static pressure due to the increase in velocity head of the gas will be relatively small. Thus, let us make the approximation that the gas flows through the discharge at constant static pressure. From the ideal gas equation ρT is a constant, and substituting into (2-6) gives:

$$\frac{\rho(\zeta)}{\rho_i} = \frac{N(\zeta)}{N_i} \simeq \frac{1}{1+\varepsilon\zeta} \tag{2-7}$$

where ρ_i is the mass density and N_i is the particle density at $\zeta = 0$, respectively. Note that the density decreases non-linearly with ζ for even this simplified case. The mass conservation requirement together with Eq. (2-7) gives:

$$\frac{v(\zeta)}{v_i} \simeq 1 + \varepsilon\zeta \tag{2-8}$$

The function $1 + \varepsilon\zeta$ and its inverse are plotted versus ζ in Fig. 4 for values of ε corresponding to a typical gas mixture and specific energy input loadings encountered in practice. The variations of the gas parameters given by the above equations can be estimated directly from these curves. For example, with a 316 j/ℓ-atm (or 300 kJ/lb) specific energy input, the temperature increases by approximately a factor of 2 and the gas density decreases non-linearly by approximately a factor of 1/2 while passing through the discharge.

There is evidence that the self-sustained glow discharge tends to operate at constant E/N with laser gas mixtures containing CO_2 because the electron losses are dominated by attachment.[3] This means that E must decrease with ζ in the same manner as N according to Eq. (2-7). Also in a constant area flow channel the glow voltage must decrease as E. We described earlier that jE must be held constant. Hence

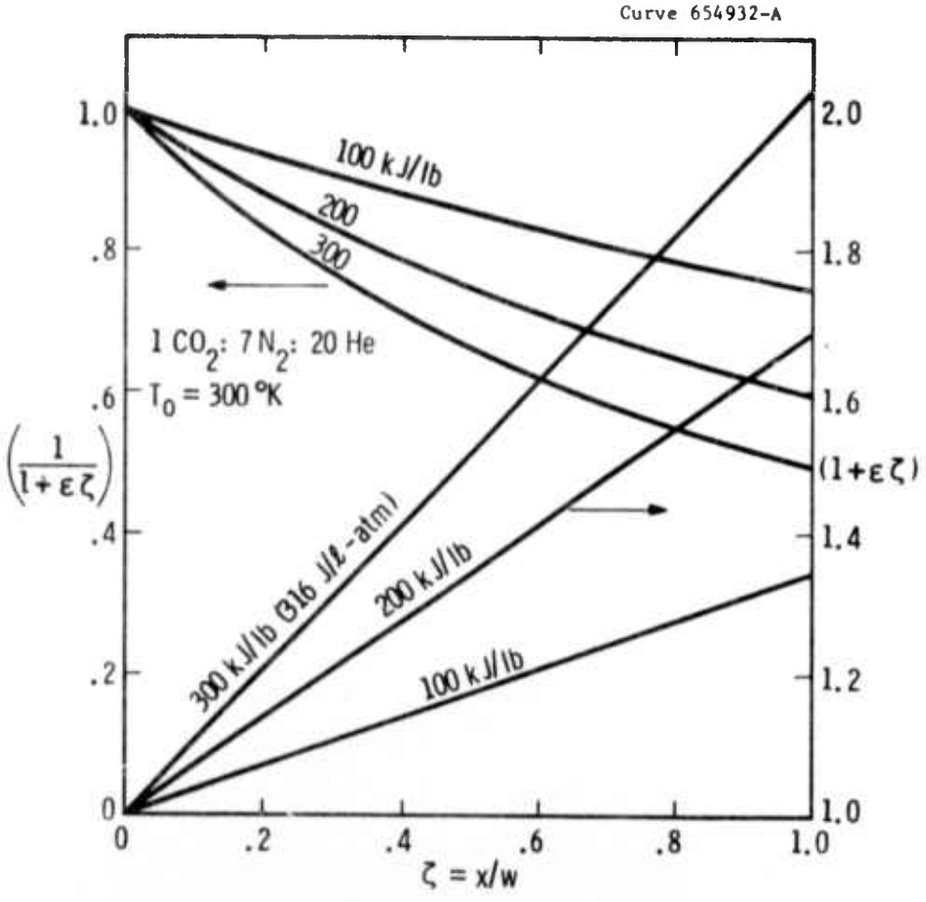

Fig. 4. Calculated values of the function $(1 + \varepsilon\zeta)$ and its inverse as a function of ζ. (See Section 2.2)

$$\frac{j(\zeta)}{j_i} \simeq 1 + \varepsilon\zeta \qquad (2\text{-}9)$$

where j_i is the current density at the upstream side of the discharge column.

The condition of linearly increasing j with ζ is readily met in the COFFEE laser scheme, at least stepwise, by adjusting the current to each row of pins in the cathode. Similarly, conditions other than constant jE could also be implemented.

2.3 Glow-to-Arc Transition

Gas flow plays a major role in permitting significant glow discharge currents at high pressures without arc formation. However, except for some limited ideas about gas heating effects producing discharge non-uniformities, there is at present little understanding of how gas flow affects arc formation.[8-10] Nevertheless, effective scaling of the discharge system requires knowing how the discharge parameters can be adjusted to increase the energy input while still avoiding arc development. To this end a computer model[11] has been developed to help clarify the potential role of gas flow and other discharge parameters in preventing arc formation. The goal of this work is to identify the important mechanisms involved in the glow-to-arc transition in order to determine how to control the discharge parameters to maintain a diffuse glow discharge.

The development of an arc from a glow discharge begins with the formation of a "precursor" channel of enhanced electrical conductivity. As the channel extends through the glow, the discharge current transfers from the diffuse portions of the glow to the path of higher conductivity, and a constricted arc eventually developes as the higher current density leads to rapid gas heating. The computer model is concerned with the axial propagation of the initial filamentary path of enhanced conductivity in a molecular gas.

In order to simplify the identification of the major discharge processes involved in arc formation, the initial stage of the work is being limited to a few specific processes without gas flow. The processes examined are selected on the basis of experimental evidence from studies of spark discharges as well as laser discharges in high-pressure gas. We have begun with gases which can dissociate but are non-attaching. (Processes involving electron attachment and detachment will be included in the near future.) We are considering a simple diatomic gas, and, at present, only thermal dissociation is included. Thus, the conductivity depends on the number densities of both the molecules and atoms, which in turn depend on gas temperature and radial convection of the gas following non-uniform gas heating.

A fairly simple model has been constructed to describe the axial propagation. The model depends primarily on the distortion of the axial electric field distribution by local increases in the electrical conductivity. This distortion leads to an increase in electric field intensity and, consequently, electrical conductivity over an extended region axially adjacent to the originally perturbed region. Thus, the region or filament of enhanced conductivity grows axially. The process can occur toward either anode or cathode, which is consistent with published experimental observations[13] as well as the experimental observations described in Section 3.2. Since it does not depend on macroscopic motions of particles, it can lead to propagation at high velocities, which is also consistent with these experimental observations.

At any instant of time in the calculations, the electric field $\vec{E}$ and the conductivity σ are related by the steady-state equation for charge conservation,

$$\nabla \cdot \left[\alpha(E)\vec{E}\right] = 0 \qquad (2\text{-}10)$$

The increased electric field intensity can cause an increase in σ in a number of ways, some of which are outlined as follows:

A. The electron temperature increases with E directly. This can cause an increase in electron mobility, but more importantly, it can increase the rate of ionization by electron impact processes.

B. Gas heating is enhanced. This increases the rate of gas expansion with a resulting decrease in gas density N and an increase in E/N. This also leads to an increase in electron temperature with the effects indicated in A.

C. Dissociation occurs at an increased rate. Under some high-pressure and high-power conditions this can be the result of thermal dissociation due to gas heating. An important effect of dissociation can be the removal of molecular (vibrational) excitation as an electron energy loss mechanism, with a resultant increase in the electron temperature and effects indicated in A. This can be a dominant effect.

The above processes have been included in the computer model, which involves two spatial dimensions (rotational symmetry assumed) and time. The calculations start out with all conditions uniform except for a localized perturbation in gas temperature (and degree of dissociation and electrical conductivity) which defines the origin of the coordinate system. The subsequent events are followed in space and time.

The explicit time dependence is contained in the gas dynamic equations which describe a compressible fluid with effects of viscosity and thermal conduction included. These equations are the conservation equations for mass, momentum, and energy, which give, respectively, the time rates of change of mass density, radial gas velocity, and gas temperature. The expressions used are given elsewhere.[12] It is assumed that all the input power is transferred from the electrons to the neutral gas which remains in thermal equilibrium at the gas temperature.

After each incremental time step in the calculations the electrical properties of the discharge are calculated from steady-state relations using the new gas properties, and the current continuity

equation is solved for the corresponding self-consistent spatial distributions of σ and E. That is, the local electrical properties are assumed to remain in equilibrium with the local properties of the neutral gas. The conductivity calculation assumes that the rate of direct ionization by electron impact is balanced by the rate of electron loss by recombination, with the electron distribution function assumed to be Maxwellian. Ionization of atoms as well as molecules is included. The conductivity is a particularly sensitive function of electron temperature, which in turn is a sensitive function of degree of dissociation. For the discharge conditions used in the calculations, the conductivity increases rapidly with dissociation.

Thus if the field increases due to the distortion, σ increases due to the dependence of electron temperature on E/N, where N decreases due to the enhanced gas heating and radial gas expansion. But more importantly, the electron temperature increases due to dissociation and the removal of molecular excitation as an electron energy loss mechanism.

In the calculations the process is initiated by introducing a perturbation in gas temperature near the origin, with the maximum temperature at the origin sufficient to cause significant ($\sim$40%) thermal dissociation. The temperature elsewhere is initially uniform and is just below the temperatures required for significant thermal dissociation.

Figure 5 shows calculated contours of electrical conductivity which indicate the time development of the filament for a small region in a diffuse nitrogen glow discharge. The initial uniform axial electric field is 10^4 V/cm, and the initial uniform current density is 10 A/cm^2. The pressure would be 300 Torr if the gas were at room temperature. The solid contours are for a value of σ 20% greater than the initial uniform value, and the dashed contours are for a value 20% less than the initial uniform value. As the region of enhanced conductivity develops along the axis, a region of depressed conductivity develops elsewhere, and as these regions develop the current shifts to the central channel at the expense of the surrounding region.

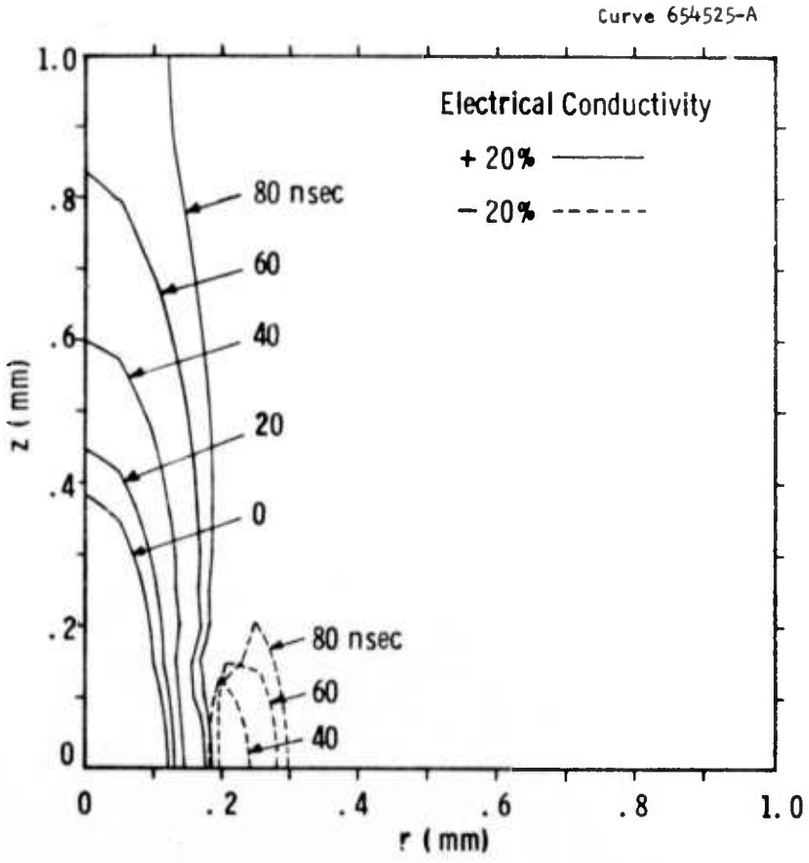

Fig. 5. Calculated spatial contours of electrical conductivity in a perturbed glow discharge with an initial uniform electrical field and current density. N_2; 300 Torr; $E = 10^4$ V/cm; $j = 10$ A/cm^2; $\sigma = 10^{-3}$ A/V^{2}cm.

The axial velocity of the leading edge of the +20% contour increases rapidly with time. After about 45 nsec it exceeds 10^6 cm/sec and continues to accelerate rapidly through t ≈ 60 nsec, at which time the leading edge leaves the region of computation. A number of other contours have also been calculated, and we find that these contours propagate at different velocities. The contours for smaller percentage changes travel faster than those for larger changes. Furthermore, calculations for a wide range of initial current densities (1 to 100 A/cm^2) indicate that the velocities are weak functions of current density.

Published experimental data on spark discharges have included measurements of axial velocities of the luminous filaments that appear as the current constricts. It is not yet clear which contour might correspond to the observed luminous filament. However, the velocities being reached by the contours are in the range of what has been measured, which is generally about 6 x 10^6 cm/sec for 300 Torr nitrogen.[13] Also, the velocity has been observed experimentally to decrease with decreasing pressure, and this trend has also been seen in the calculations.

The calculated results so far are preliminary, and the comparison with experiment can be made only qualitatively. Nevertheless, it does appear that the mechanisms considered, that is, field distortion followed by locally enhanced gas heating and dissociation, can be important in the formation of a filamentary arc in a diffuse, molecular glow discharge. Dissociation appears to be especially important, since it can lead to significant increases in electron energy and in the ionization rate.

The emphasis has been on the propagation of the conducting filament once it is initiated. Both the initiation conditions and the propagation across the discharge gap are necessary for an arc to develop, and the obstruction of either of these requirements is sufficient to prevent an arc from forming. The present results suggest, for example, that for a dissociating (non-attaching) gas the local electron temperature and conductivity variations might be retarded by the introduction of a gas component with molecular excitation energies somewhat greater than those of the primary gas. Then when the primary species dissociates, the electron energy losses do not decrease abruptly.

The calculations also suggest that a major role of gas flow might be to prevent the initial filaments of relatively small conductivity changes from crossing the discharge gap, even when the onset conditions are present. This might occur by direct gas cooling or by turbulence effects. The result might be that the precursors to the luminous arcs, which apparently cross the gap well before the luminous stage appears experimentally, are prevented. This should prevent arcs from forming in spite of the existence of high local gas temperatures or hot-spots near the electrodes.

3. GLOW DISCHARGE EXPERIMENTS

3.1 Electrode Module (10 x 10 x 10 cm) Studies

As part of the COFFEE laser study program an electrode module was designed, built, and tested in order to determine glow discharge scalability as a function of the important parameters. One important purpose of the module experiments was to demonstrate the feasibility of building a large-scale laser device. In addition, parametric studies have been started to determine the influence of the main parameters, such as discharge current, gas velocity, pressure, mixture and cathode pin spacing. In the future small signal gain measurements will be made as a function of these variables to determine the uniformity and efficiency of the excitation. These experiments have also been providing important information for the theoretical models of the glow discharge and laser excitation phenomena.

3.1.1 Description of Discharge Module

The discharge module forms a two-dimensional flow nozzle (subsonic) which consists of a planar anode on one side and a sheet of high-temperature dielectric on the other side. The two electrodes are shown in Figs. 6-7. The cathode consists of a multipin array (110 pins) protruding through the insulating sheet with a pin density of 1 pin/cm^2. Looking along the 10 cm optical axis, transverse to the flow, one sees 11 rows of 10 pins. Each pin in a given row is connected through a separate 50 kΩ ballast resistor to a common row bus bar. As the laser gas passes from row to row, the discharge impedance lowers due to gas heating as explained in Section 2.2. This is compensated in the present case by adding a separate ballast resistor to each row in order to maintain a nearly constant input power density. A diverging flow channel could also have been used.

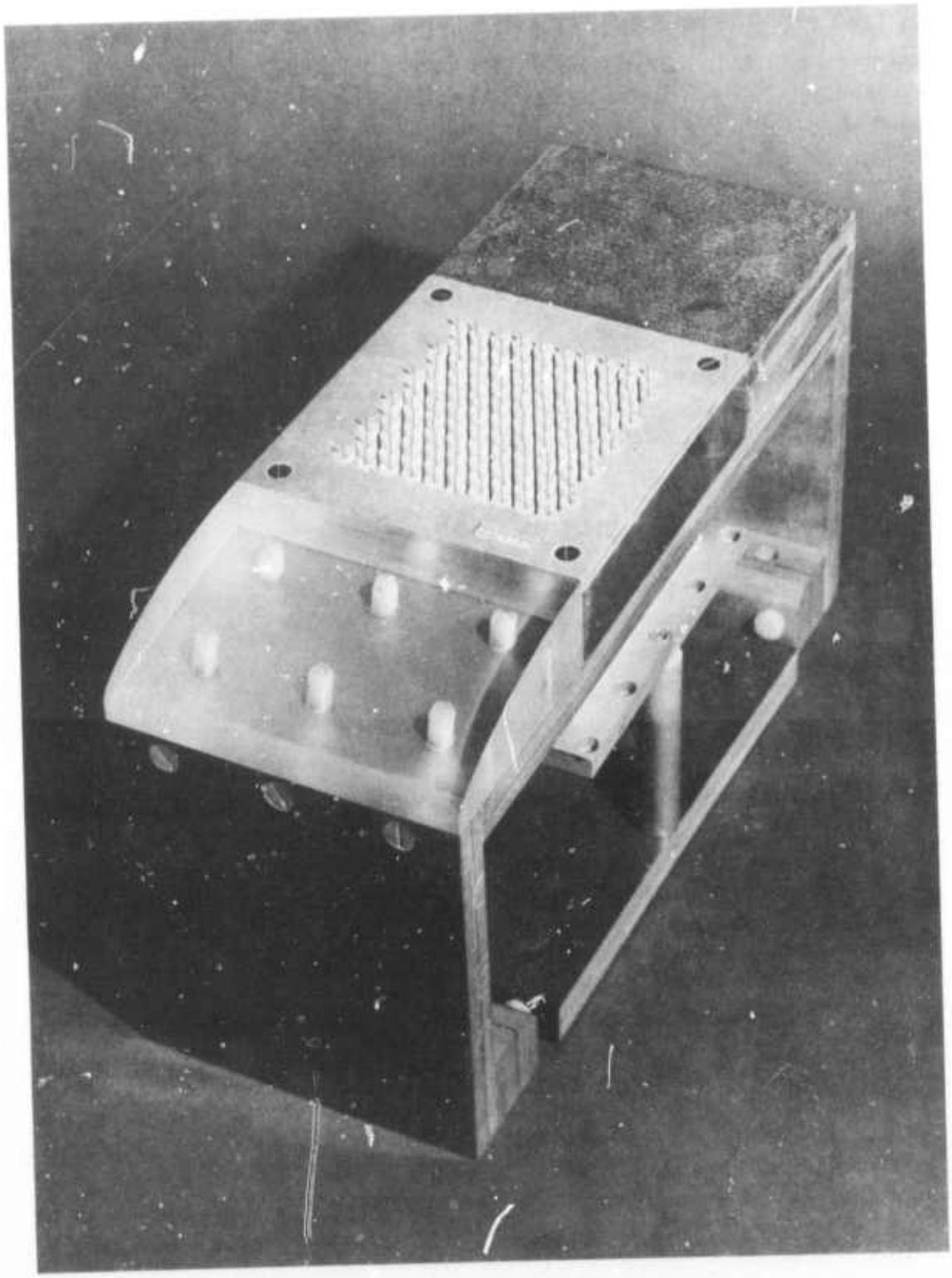

Fig. 6. Multipin cathode assembly.

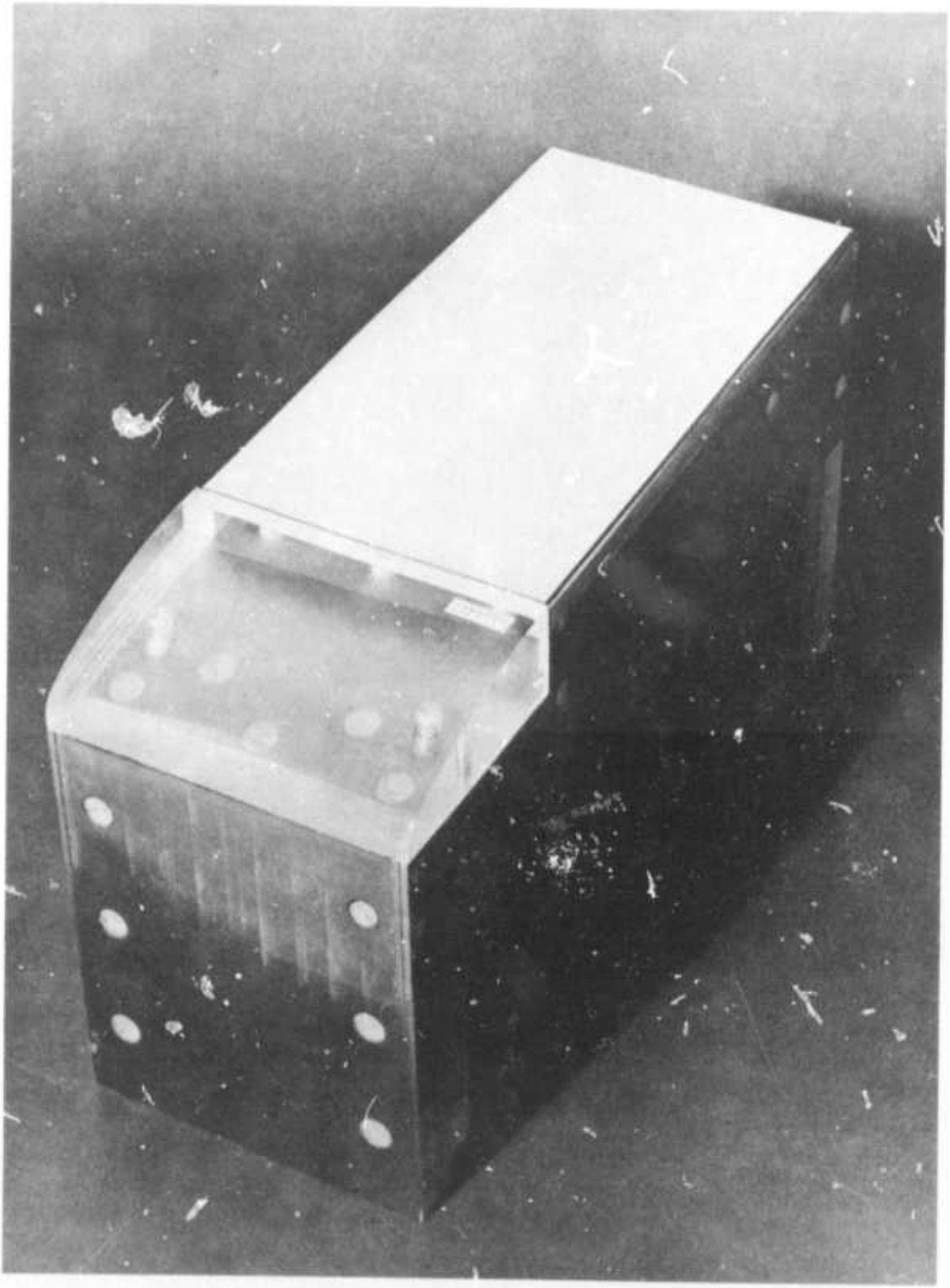

Fig. 7. Anode assembly.

The electrode gap is variable from 2 to 10 cm. The distance between the first and last row of cathode pins is 10 cm. Alternate rows are staggered with respect to the gas flow so that the nearest downstream pin is 2 cm away, minimizing the discharge interactions. Tungsten pins with a 1 mm diameter and a sharp conical tip are used. The copper anode is 15 cm wide and approximately 30 cm long. All the sharp edges are removed from the anode.

The electrodes are fitted into a special vacuum-tight fiberglass test section housing (see Fig. 8). This construction maintains pure gas conditions while eliminating possible arc-over problems. The test section is part of a closed-loop wind tunnel capable of operating at any pressure up to 1 atm with variable flow rates up to 170 m^3/sec.

3.1.2 Experimental Results

The high-pressure direct current self-sustained glow discharge has been successfully scaled to a 10 cm square aperture. A photograph of the glow discharge is shown in Fig. 9. On visual examination the glow appears fairly uniform. The glow is less visible under the first two rows because the current to these rows was less than to the other rows. The upstream rows act to condition or preionize the gas for the downstream rows which are then able to carry more current without arcing.

In the first experiments, input power densities up to 50 W/cm^3 of discharge volume were obtained with a specific input energy of 115 J/ℓ-atm (∿110 kJ/lb). It is expected that this value will be raised to greater than 200 J/ℓ-atm in subsequent tests after the operating parameter optimization has been completed, because such values were achieved in small-scale tests previously.[14]

Since the construction of the discharge module was completed only recently as per schedule, the range of parameters studied is rather limited to date. For example, the gas pressure range studied has been between 70 and 300 Torr where larger variations in useful discharge current are presently achievable. Only a few gas velocities and row ballast arrangements were tried. Some difficulty was experienced with

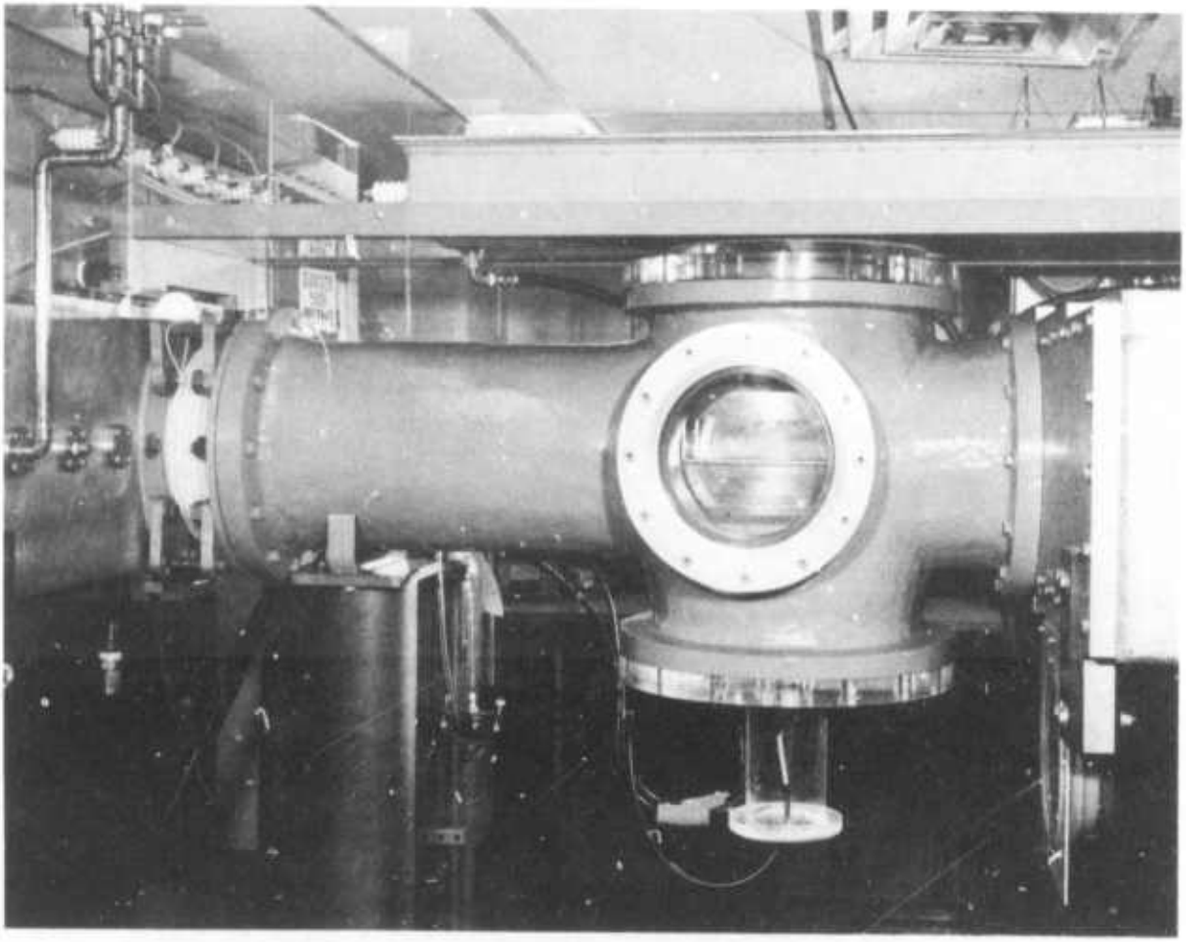

Fig. 8. Fiberglass test section housing with anode and cathode assemblies installed.

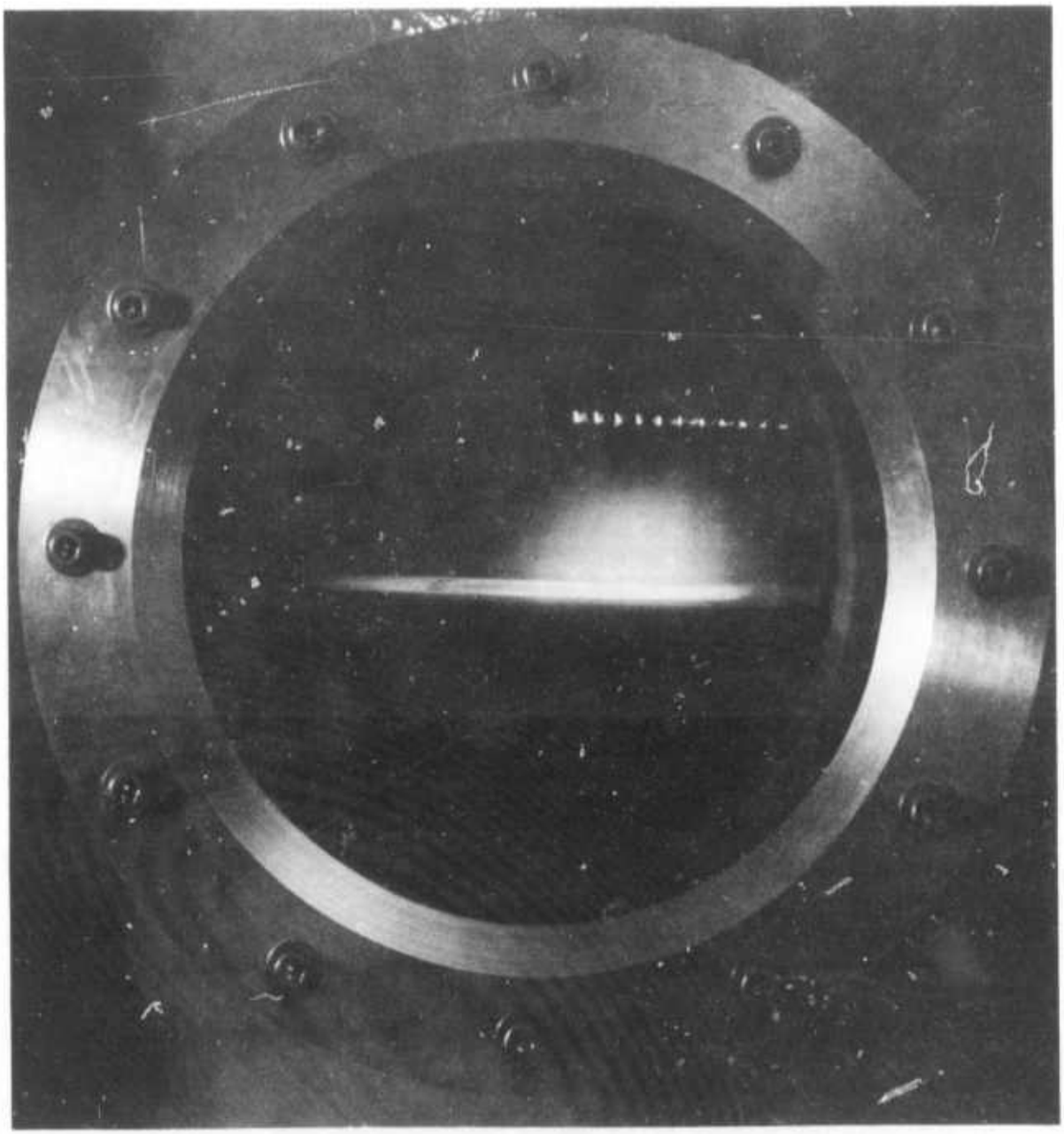

← Flow 150 m/sec

Fig. 9. High-pressure dc glow discharge viewed along optical axis of 10 x 10 x 10 cm module. 140 Torr; $1CO_2$:$7N_2$:20He.

the initial anode design at the larger electrode spacings (8-10 cm). The ratio of anode width to gap size was purposely kept small (1.5 to 1 with 10 cm gap) to minimize the amount of cold gas by-passing the sides of the discharge. This produced a field enhancement at the lateral edges of the anode which caused breakdown to these edges when the input power density was raised to $\sim$20 W/cm^3. With electrode gaps smaller than 6 cm where edge effects were absent, 40-50 W/cm^3 were routinely obtained. The anode is presently undergoing modification to eliminate the field enhancement problem.

A typical set of V-I curves for the parallel glow discharges are shown in Fig. 10. The six solid curves each connect the data points common to a particular row ballast resistor. For example, rows 2 and 3 share a common row resistor, rows 4 and 5 share another row resistor, and so forth. (In later experiments each row has its own ballast resistor.) The V-I characteristics in Fig. 10 are coupled because the upstream rows affect the downstream rows. The five data points on each line correspond to one of five total current settings. For example, the points furtherest to the right on each curve were all measured simultaneously and were obtained at the maximum current setting.

In general terms Fig. 10 shows that the glow voltage is nearly independent of discharge current. Also the glow voltage decreases in the downstream direction due to gas heating. At maximum power input, all except the first row is dissipating about the same power per unit discharge volume because the values of row ballast resistance in use at the time are nearly optimum for these conditions. Unfortunately, if one were to change the size of the resistor in row 1, all the other curves would be shifted to higher or lower values of glow voltage due to the resultant change in gas heating by row 1. Thus, the data in Fig. 10 only apply to one specific set of conditions.

A more universal approach to analyzing the V-I characteristics is obtained by following the type of analysis presented in Sections 2.1 and 2.2. The current density, gas density, and input power density are plotted in Fig. 11 against the normalized distance along the flow path for a particular set of operating conditions. The current density in a row is

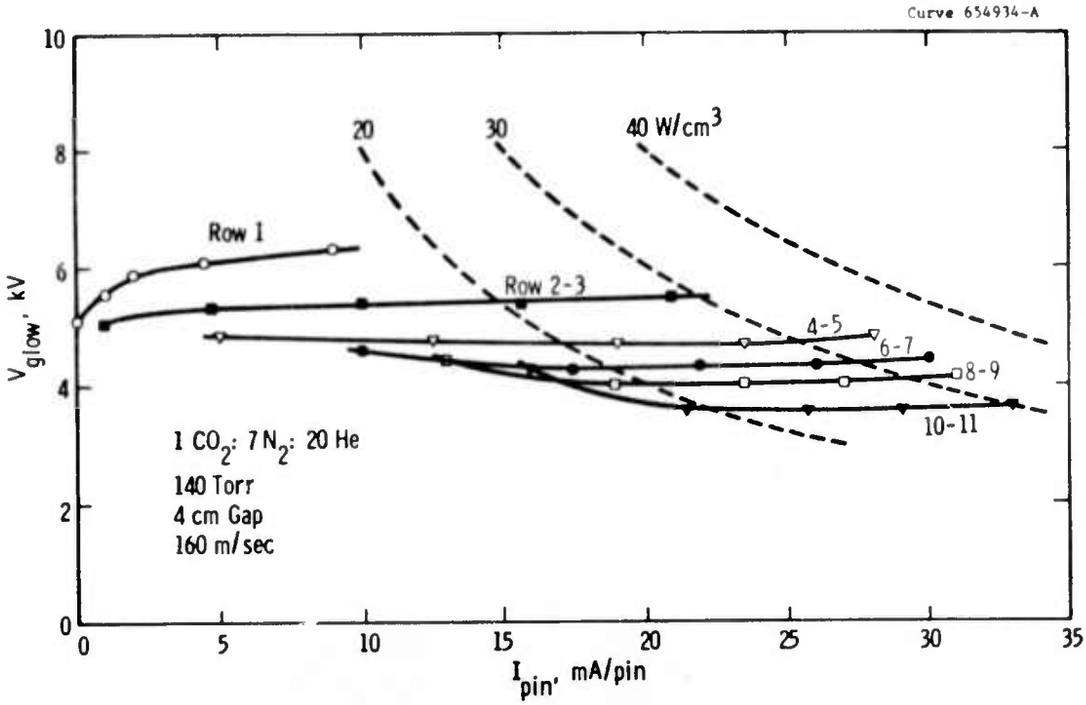

Fig. 10. Measured V-I characteristics for cathode pin rows indicated.

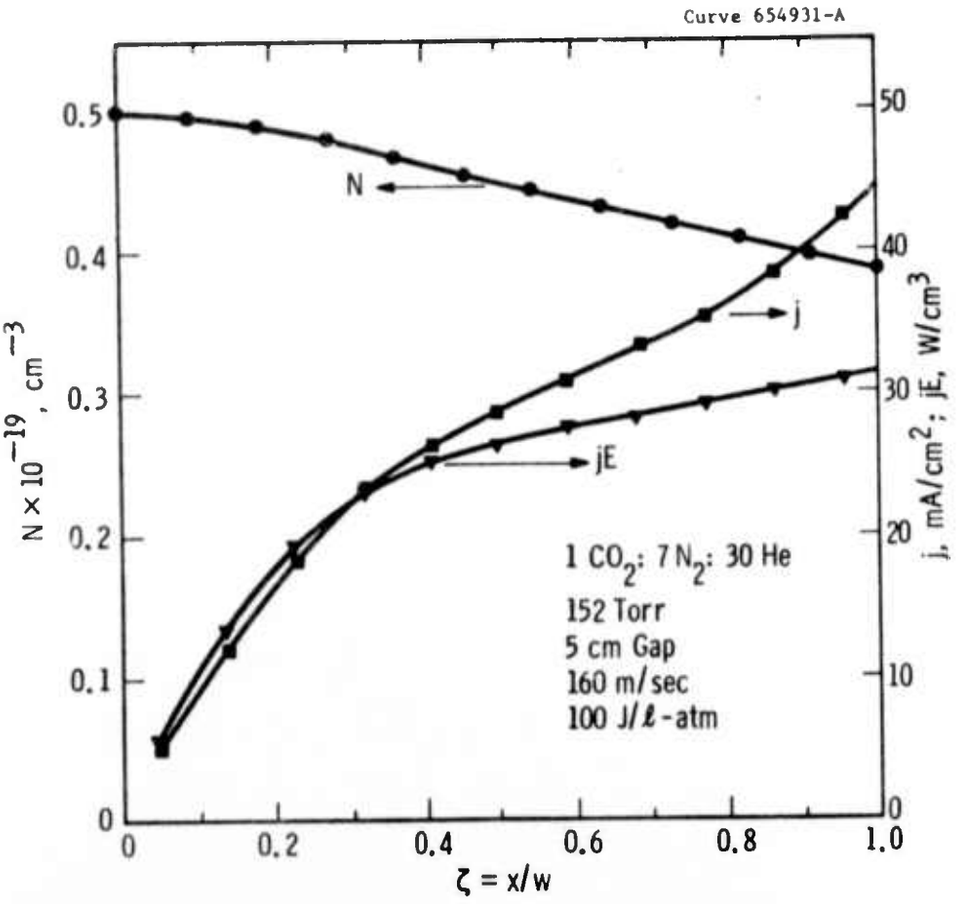

Fig. 11. Measured gas density, current density, and input power density as a function of normalized distance along gas flow path.

defined as the total current to the row divided by the number of cathode pins per row (10 pins) and the average pin density (1 pin/cm^2). For this test condition the current density increases by a factor of 9 between the upstream and downstream rows. A higher value of j in the first 3 or 4 rows would have made the input power density, jE, more uniform.

The electric field is computed by subtracting 500 volts from the measured glow voltage, which allows for the electrode fall voltages,[14] and then dividing this value by the electrode gap. Next, one can calculate the local (row) jE values. With jE known, one then calculates the local gas temperature rise for the given gas flow rate and composition. Next, one computes the distribution of local gas density, assuming an ideal gas, as shown in Fig. 11. Although the gas density decreases overall by approximately 25% as predicted by Fig. 4 in passing through a discharge with a specific power of 100 J/ℓ-atm, the density distributions are different. This is because the input power density distributions are not the same.

Once E, j, and N are known, the operating E/N can be calculated as a function of j/N as shown in Fig. 12. The resulting E/N is almost constant throughout the discharge. The data seem to indicate a slight decrease in E/N as the gas heats up. This may be due to certain discharge products being carried downstream. On the other hand, the trend is within the uncertainty of the limited amount of data, and no definite conclusion can be drawn on this point. The resulting E/N agrees with the value predicted by Lowke[3] and the value measured by Denes[4] in a pulsed discharge for a 1:7:30 mixture (see Fig. 3). Since the E/N in Fig. 12 is essentially constant for more than a factor of 10 change in j/N, it appears that our continuous, self-sustained glow discharge is attachment controlled under the present operating conditions.

The cathode pin density of 1 pin/cm^2 was chosen on the basis of previous experience[14] as a reasonable starting point. The effective pin density can be decreased by disconnecting some of the pins or rows of pins. Preliminary results show that the same amount of power can be put into the discharge volume of the module with every other row of pins disconnected. The discharge is not as uniform in this case.

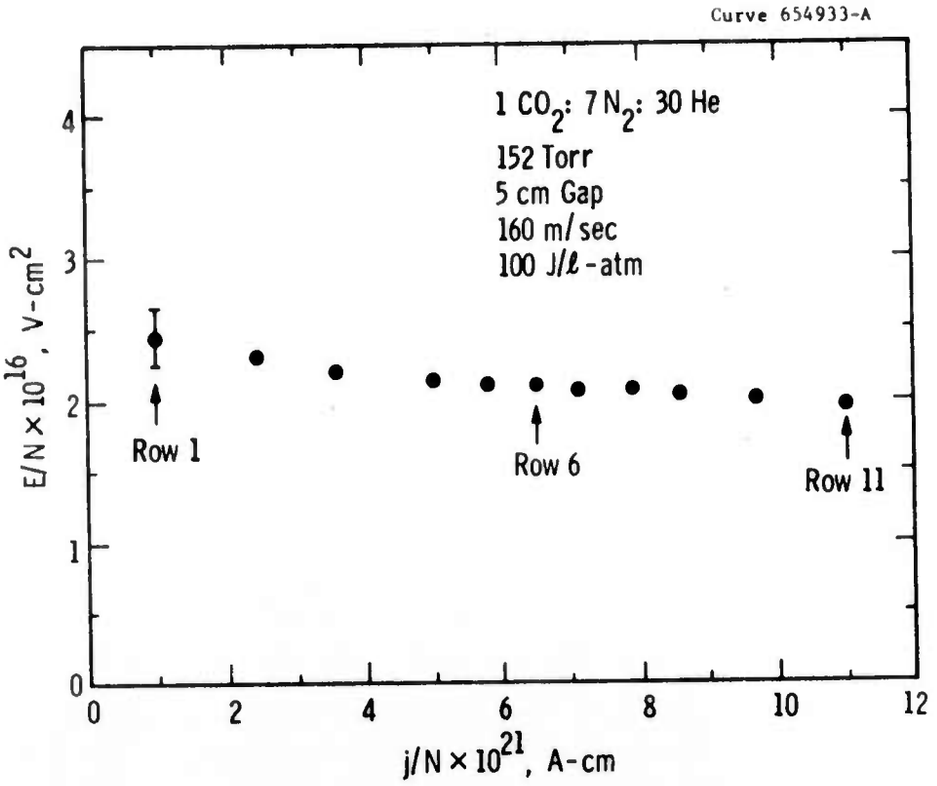

Fig. 12. Measured E/N as a function of j/N distribution along gas flow path.

The pin density is also constrained by the maximum current that can be drawn without arcing from each cathode pin under various operating conditions. For example, at p = 280 Torr with a 1:7:20 gas mixture traveling at 150 m/sec, over 100 mA can be passed through a single pin-to-plane discharge with a 4 cm electrode gap. When a single row of pins with a 1 cm transverse spacing is inserted into this same gas flow field, only 35 mA/pin is obtainable. Yet, it is possible to obtain over 50 mA/pin from this same row of pins if another row of pins is activated upstream from it at a somewhat lower current level. This indicates that the upstream discharges tend to favorably "condition" the gas for the downstream discharges.

There is some question about the validity of extrapolating the single pin data to a large number of pins. When large currents are drawn from a single pin, the discharge current tends to start fluctuating. Although arcs are not observed and the glow voltage does not collapse, apparently partial arc-overs in the form of short, highly conducting filaments are occurring in the vicinity of the cathode which effectively form a large area "virtual cathode" (see Section 3.2). This virtual cathode is then able to supply the current equivalent of 2 or 3 closely spaced pins operating under the usual glow conditions. The virtual cathode mode of operation does not seem to extend stably to multi-cathode electrode configurations, even with relatively large (2 cm) inter-cathode spacings. Also, laser gas degradation is observed in this operating regime, much like that experienced if the discharge is allowed to arc frequently, and this is, of course, undesirable.

If one increases the pin density, there seems to be an upper limit to the maximum current density, based on the area of the discharge column, which can be obtained before arcing will occur. Adding more cathode pins just lowers the current per pin required to achieve this threshold current density and makes the cathode more complex to build. In general, the row-to-row discharge interactions will require more study before the optimum cathode pin density can be determined.

No systematic study of gas degradation effects was included in this program. However, it has been observed that there are no problems if arcing is avoided. As reported earlier,[14] the discharge can be run for over one hour in a closed-loop flow system without any make-up gas, and no significant changes, such as build up of CO or NO_x and increased operating voltage, are observed. On the other hand, we have found that the glow voltage does increase with time if the discharge is operated for an extended period just below the current limit for arcing. Furthermore, the current threshold for arcing gradually lowers. These results suggest that the gas is slowly decomposing due to partial arc-overs which may be occurring when operating just below the current limit that leads to a complete arc transition with a collapse of the glow voltage.

Visually the axis of the glow discharge column appears to be deflected downstream with respect to the cathode by approximately 15-30 degrees, depending on the flow velocity. With spacings up to 10 cm there is no problem with the glow blowing out or becoming positionally unstable for gas velocities up to 150 m/sec. More will be learned about the distribution of the glow current when the small signal gain measurements are made.

3.2 Glow-to-Arc Experiments

One of the main bodies of information needed for developing a COFFEE laser scaling criteria is an understanding of the glow stability. We know that gas flow is required to operate the self-sustained glow continuously at high pressures and reasonable power levels. The discharge physics of the glow stabilization, however, is poorly understood.[8-10] In order to gain more insight into conditions leading to arcing, a single-pin-to-plane discharge was studied in a transverse flow field using a small-scale, closed-loop flow system. The test section was designed with a transparent wall for viewing the discharge photographically. It is recognized that the study of a single cathode pin leaves out multipin interactions, such as pin-to-pin arcs, simultaneous or parallel

arcs, and preconditioning effects from upstream glows. On the other hand, it is too difficult in the beginning to isolate detailed arc formation phenomena in the more complex situations.

At the present time these investigations have proceeded to the point where we can give a brief phenomenological description of the glow-to-arc transition for our geometry. Figure 13 is a photograph of a 60 mA glow where one arc transition occurred during the 15 second exposure period. The operating conditions were: p = 140 Torr, $1CO_2$: $7N_2$:20He:$0.4H_2$, and gas velocity = 60 m/sec. The glow voltage was 4900 volts.

The glow is composed of several distinct regions. The brightest is the cathode glow in the sheath which covers almost all of the 1.6 cm x 1.5 mm diameter tungsten pin. The positive column, which is just barely visible, spreads out towards the anode and is slightly deflected by the gas flow. A bright fan-shaped plume extends downstream from the cathode at high current levels even if arc transitions are not occurring. The plume seems to have a lower electrical conductivity than the column. The thin, curved arc channel shown in Figure 13 always occurs on the downstream side of the glow where the gas is hottest. In all the cases described in this section the discharge electrodes had an RC circuit, consisting of an 0.05 μF capacitor in series with a 2000 Ω resistor, connected in parallel with them. This increased the glow instability for study purposes and increased the arc transition intensity for photographic purposes. The RC time constant limited the arc duration to approximately 100 μsec in Fig. 13. This means that there could only have been a small displacement of the arc during its existence, and that the run-away portion of the arc transition had to occur near the location shown. The fuzziness of the downstream side of the arc indicates that the channel may have moved a little as the current decayed.

There are some operating conditions in which highly luminous filaments extend 2 to 3 cm downstream from behind the cathode plume, but fade out and do not appear to cross the electrode gap. This corresponds to the "partial arc-over" described in the Section 3.1.2.

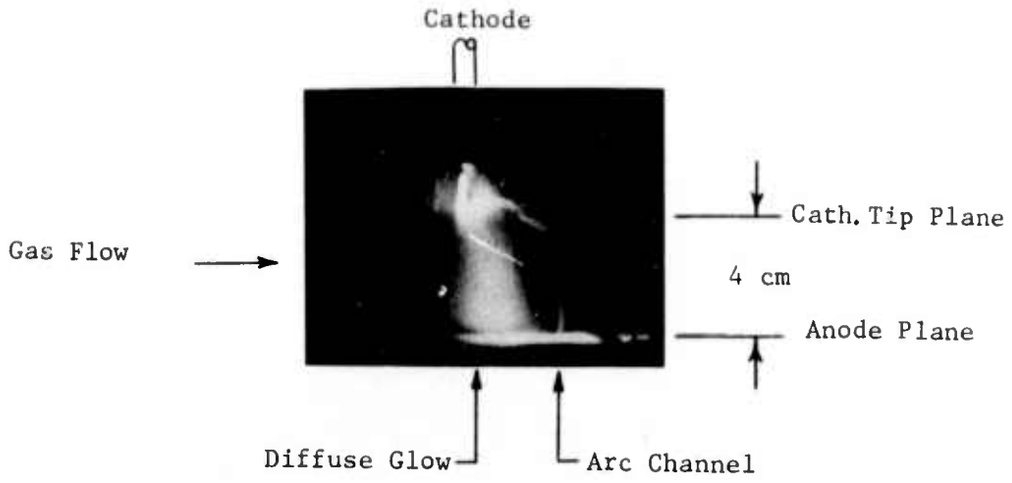

Fig. 13. A 15 sec. exposure of glow discharge showing one glow-to-arc transition.

The onset of arcing correlates with the development of relatively large fluctuations in the discharge current. For example, while operating at 100 mA average current, occasional current pulses as high as 400 mA would occur without causing an arc. These pulses approximated half of a sine wave with a half-period of about 1 ms. The energy in such a pulse is about 1 Joule. If this energy is deposited in only part of the total discharge volume due to local perturbations in the conductivity as suggested in Section 2.3, the local gas temperature could rise several hundred to several thousand degrees.

If the spurious current pulse exceeded 400 mA for the given operating conditions, a faint precursor filament was observed on the photographs along a path typified by the arc channel in Fig. 13. This was followed by a rapid increase in current, a collapse of the discharge voltage, and an increase in the filament luminosity. This latter process only takes a few μsec to occur as shown in Fig. 14 which is a 7 μsec streak photograph of the phenomena taken with an STL camera. After the faint precursor is formed, time t = 0 in the streak photograph, a highly luminous region travels in a wave-like manner away from the cathode along the path of the precursor. As soon as this wave turns the corner and starts toward the anode, a second wave of high luminosity leaves the anode and travels toward the cathode along the precursor path. When the two waves meet approximately at the middle of the electrode gap, this region momentarily gets very bright. Then the luminosity fades to an intermediate value and becomes uniform along the arc channel. The onset of the bright waves corresponds to the sudden increase in current growth rate when $I > 400$ mA. When the two waves meet, the current has increased to approximately one-half of its final value and the discharge voltage has collapsed half-way. This corresponds to the maximum instantaneous input power condition. These two approaching waves are the two intersecting bright lines in Fig. 15. The slopes of these lines give a maximum velocity of $\sim 10^6$ cm/sec which is consistent with the results in Section 2.3. The momentary bright region which occurs when the waves meet is also shown in the middle frame of Fig. 15. These three

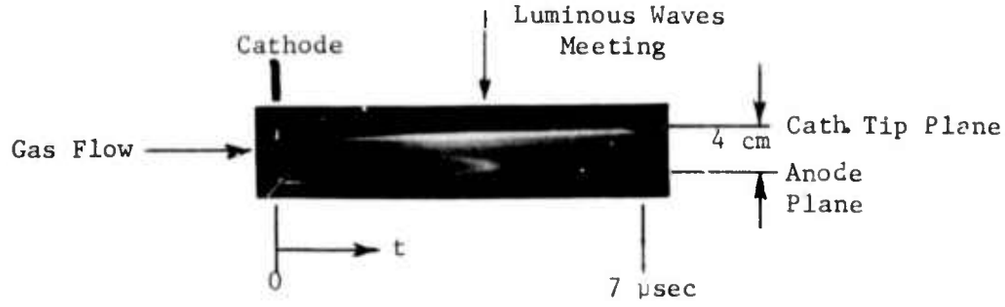

Fig. 14. Double exposure showing glow discharge at t = 0 and superimposed 7 μsec streak photograph of glow-to-arc transition.

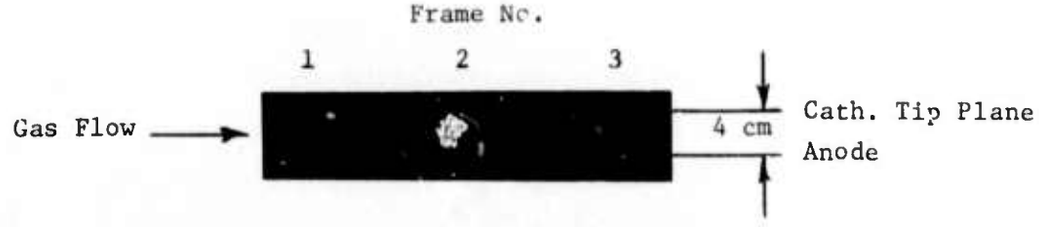

Fig. 15. Frame pictures of glow-to-arc transition. Exposure = 200 nsec; time between frames = 5 μsec.

photographs have 200 nsec exposures and were taken 5 μsec apart using the framing mode of an STL image converter camera. The first frame shows the faint precursor just before the voltage collapse when the current was approximately 400 mA. The second frame was taken at I = 1.4A, just past the half-way point, and the last frame was taken at I = 2.4A approximately 4 μsec after the arc transition was complete. Thus, the glow-to-arc transition seems to consist of a relatively slowly developing precursor filament having a conductivity somewhat greater than the surrounding glow. This precursor suddenly becomes unstable and develops into a highly conducting arc channel.

It is assumed on the basis of our present knowledge that the gas flow stabilizes the glow discharge by inhibiting the formation of the precursor filaments. The characteristic gas transit times are of the same order as the apparent precursor formation times. The highly conducting arc channel forms too fast for the gas flow to directly influence it. Future work must be directed towards understanding the influence of gas flow and other processes on the energy balance which presumably governs the formation of arc precursors.

4. RECOMMENDATIONS

The scaling criteria for the COFFEE laser excitation scheme are at present incomplete. It is recommended, therefore, that the scaling studies be continued in order to obtain a more definitive evaluation of scalability. Several specific areas need further investigation. First, the discharge parameterization experiments should be completed. Not only are better optimized operating conditions needed, but also the functional dependencies of the various design parameters on the operational parameters must be determined more completely. For example, the specific input power and input power density are both limited by discharge instability. Thus, the glow stability limits need to be determined as a function of the primary variables, such as gas velocity, gas density, current density, cathode pin density, electrode separation, and gas composition. The glow-to-arc analytical modeling needs to be extended to include such processes as electron attachment and detachment. Gas flow effects also need to be considered in greater detail.

Second, more information is needed for optimizing the cathode pin density and array design criteria. Cathode pin interaction phenomena require clarification. Further row and pin ballast resistor optimization would be useful.

Finally, small-signal gain measurements of the excited media should be made. These measurements would determine the excitation efficiency as a function of the operational parameters and should be correlated with our existing laser and discharge kinetics codes.[15] The uniformity of the excitation also needs to be verified.

With all this information it should be possible to formulate a fairly comprehensive discharge scaling criteria. This could be used to design simple, rugged, and compact high-power laser systems.

5. REFERENCES

1. W. L. Nighan and J. H. Bennett, Appl. Phys. Lett. 14, 240 (1969).
2. J. J. Lowke, A. V. Phelps and B. W. Irwin, J. Appl. Phys. 44, 4664 (1973).
3. J. J. Lowke and L. J. Denes, Paper FB-2, 26th Gaseous Electronics Conference, Madison, Wis., October, 1973).
4. L. J. Denes and J. J. Lowke, Appl. Phys. Lett. 23, 130 (1973).
5. F. C. Fehsenfeld, E. E. Ferguson, and A. L. Schmeltckopf, J. Chem. Phys. 45, 1844 (1966).
6. J. L. Moruzzi and A. V. Phelps, J. Chem. Phys. 45, 4617 (1966).
7. A. H. Shapiro, The Dynamics and Thermodynamics of Compressible Flow, Vol. I, Ronald Press, New York (1954).
8. Yu S. Bortnikov, et al., Soviet Physics 14, 1579 (1970).
9. R. McLeary and W. E. K. Gibbs, IEEE Jrnl. of Quantum Electron. QE-9, 828 (August, 1973).
10. T. F. Deutch, F. A. Horigan, and R. I. Rudko, Appl. Phys. Lett. 15, 88 (August, 1969).
11. G. L. Rogoff, Paper AA-8, 26th Annual Gaseous Electronics Conference, Madison, Wisconsin (October, 1973).
12. G. L. Rogoff, Phys. Fluids 15, 1931 (1972). Note that the mass conservation equation is given in terms of particle number density in this reference, which does not include calculations of dissociation. For the present calculations the number density is replaced by mass density.
13. I. D. Chalmers, H. Duffy, and D. J. Tedford, Proc. R. Soc. Lond. A. 329, 171 (1972).
14. S. A. Wutzke and J. L. Pack, Conf. on Laser Engrg. and Applications, Washington, D. C. (1973).
15. Westinghouse Research Memo 73-1C8-SHOWA-M1.

UNCLASSIFIED

SECURITY CLASSIFICATION OF THIS PAGE *(When Data Entered)*

REPORT DOCUMENTATION PAGE		READ INSTRUCTIONS BEFORE COMPLETING FORM
1. REPORT NUMBER NONE	2. GOVT ACCESSION NO.	3. RECIPIENT'S CATALOG NUMBER
4. TITLE *(and Subtitle)* CW PIN DISCHARGE LASER		5. TYPE OF REPORT & PERIOD COVERED Final Technical Report 15 March 73 - 14 Sept. 73 6. PERFORMING ORG. REPORT NUMBER
7. AUTHOR(s) S. A. Wutzke, J. L. Pack, G. L. Rogoff, J. J. Lowke		8. CONTRACT OR GRANT NUMBER(s) N00014-73-C-0318
9. PERFORMING ORGANIZATION NAME AND ADDRESS Westinghouse Electric Corporation Research Laboratories Pittsburgh, Pennsylvania 15235		10. PROGRAM ELEMENT, PROJECT, TASK AREA & WORK UNIT NUMBERS Program Code 3E90
11. CONTROLLING OFFICE NAME AND ADDRESS Procuring Contracting Officer Office of Naval Research Department of the Navy Arlington, Va. 22217		12. REPORT DATE November 14, 1973 13. NUMBER OF PAGES 37
14. MONITORING AGENCY NAME & ADDRESS*(if different from Controlling Office)* Commander, Defense Contract Administration Services District 1610-S Federal Bldg., 1000 Liberty Avenue Pittsburgh, Pa. 15222		15. SECURITY CLASS. *(of this report)* UNCLASSIFIED 15a. DECLASSIFICATION/DOWNGRADING SCHEDULE NA
16. DISTRIBUTION STATEMENT *(of this Report)* ONR Distribution List Attached		
17. DISTRIBUTION STATEMENT *(of the abstract entered in Block 20, if different from Report)*		
18. SUPPLEMENTARY NOTES ARPA Order No. 1806, Amed. #9, dtd. 11-15-72		
19. KEY WORDS *(Continue on reverse side if necessary and identify by block number)* lasers, glow, scaling, breakdown, discharges, sparks, pins		
20. ABSTRACT *(Continue on reverse side if necessary and identify by block number)* The results of a study program on a Continuously Operating Fast Flow Electrically Excited (COFFEE) laser excitation concept are reported. The concept uses a multipin-to-plane electrode configuration with transverse gas flow to produce a high-pressure, self-sustained glow discharge. Emphasis is placed on developing the glow discharge scaling criteria. Both theoretical and experimental studies of the glow discharge characteristics, input power distribution, and glow-to-arc transition phenomena are described.		

DD FORM 1 JAN 73 1473 EDITION OF 1 NOV 65 IS OBSOLETE

UNCLASSIFIED

SECURITY CLASSIFICATION OF THIS PAGE *(When Data Entered)*

The high-pressure continuous glow was successfully scaled experimentally to a 10 cm square aperture. The excitation concept looks attractive for high-power laser devices.